Pergamon

Geochimica et Cosmochimica Acta, Vol. 67, No. 9, pp. 1699–1709, 2003

0016-7037/03 $30.00 + .00

doi:10.1016/S0016-7037(02)00026-7

The distribution of sodium ions in aluminosilicate glasses: A high-field Na-23 MAS and 3Q MAS NMR study

SUNG KEUN LEE* and JONATHAN F. STEBBINS

Department of Geological and Environmental Sciences, Stanford University, Stanford, CA 94305-2115, USA

(*Received May* 22, 2002; *accepted in revised form October* 22, 2002)

Abstract—The local configurations around sodium ions in silicate glasses and melts and their distributions have strong implications for the dynamic and static properties of melts and thus may play important roles in magmatic processes. The quantification of distributions among charge-balancing cations, including Na^+ in aluminosilicate glasses and melts, however, remains a difficult problem that is relevant to high-temperature geochemistry as well as glass science.

Here, we explore the local environment around Na^+ in charge-balanced aluminosilicate glasses (the $NaAlO_2$-SiO_2 join) and its distribution using ^{23}Na magic-angle spinning (MAS) nuclear magnetic resonance (NMR) spectroscopy at varying magnetic fields of 9.4, 14.1, and 18.8 T, as well as triple-quantum (3Q)MAS NMR spectroscopy at 9.4 T, to achieve better understanding of the extent of disorder around this cation. We quantify the extent of this disorder in terms of changes in Na-O distance (d[Na-O]) distributions with composition and present a structural model favoring a somewhat ordered Na distribution, called a "perturbed" Na distribution model. The peak position in ^{23}Na MAS spectra of aluminosilicate glasses moves toward lower frequencies with increasing Si/Al ratios, implying that the average d(Na-O) increases with increasing R. The peak width is significantly reduced at higher fields (14.1 and 18.8 T) because of the reduced effect of second-order quadrupolar interaction, and ^{23}Na MAS NMR spectra thus provide relatively directly the Na chemical shift distribution and changes in atomic environment with composition. Chemical shift distributions obtained from ^{23}Na 3Q MAS spectra are consistent with MAS NMR data, in which deshielding decreases with R. The average distances between Na and the three types of bridging oxygens (BOs) (Na-{Al-O-Al}, Na-{Si-O-Al}, and Na-{Si-O-Si}) were obtained from the correlation between d(Na-O) and isotropic chemical shift. The calculated d(Na-{Al-O-Al}) of 2.52 Å is shorter than the d(Na-{Si-O-Si}) of 2.81 Å, and d(Na-{Al-O-Al}) shows a much narrower distribution than the other types of BOs. ^{23}Na chemical shifts in binary (Al-free) sodium silicate glasses are more deshielded and have ranges distinct from those of aluminosilicate glasses, implying that d(Na-NBO) (nonbridging oxygen) is shorter than d(Na-BO) and that d(Na-{Si-O-Si}) in binary silicates can be shorter than that in aluminosilicate glasses. The results given here demonstrate that high-field ^{23}Na NMR is an effective probe of the Na^+ environment, providing not only average structural information but also chemically and topologically distinct chemical shift ranges (distributions) and their variation with composition and their effects on static and dynamic properties.

1. INTRODUCTION

Essential to the macroscopic thermodynamic and transport properties of aluminosilicate melts and glasses is the full understanding of the atomic arrangements and the extent of disorder among atoms. Recent quantification of the disorder and site connectivity among framework cations and oxygens in aluminosilicate and borosilicate glasses using nuclear magnetic resonance (NMR) spectroscopy allowed us to evaluate the extent of disorder in terms of the degree of Al avoidance (Q) and degree of phase separation (P) and provided improved understanding of the configurational properties of corresponding melts (Lee and Stebbins, 1999, 2000a, 2000b; Lee et al., 2001). Therefore, we can now determine the distribution of framework cations and anions in some classes of network structured glasses and are able to predict the extent of disorder and the microscopic origin of macroscopic properties and how they change with temperature and composition (Lee and Stebbins, 2002).

In spite of these advances, the distributions of non-network-forming cations, such as Ca^{2+} and Na^+, are still poorly known and remain controversial (e.g., random or clustered, coordination number [CN], etc.) (Gaskell et al., 1991; Jund et al., 2001). The local configurations around those cations are important because several fundamental properties of glass-forming liquids, including viscosity and the diffusion through the network, are affected by their local coordination and their bonding with the framework. For example, Na-O distance is one of the key factors in controlling the Na transport through the percolation channels or among available hopping sites for Na (Houdewalter et al., 1993). The extent of disorder in nonnetwork cations also has strong implications for the intermediate structure. However, despite various efforts to determine the local configuration of nonnetwork cations in aluminosilicate glasses, estimates of the CN of Na^+ and its compositional dependence vary from 5 to 8 depending on the spectroscopic method used. For example, Na k-edge extended X-ray absorption fine structure (EXAFS) studies of binary sodium silicate glasses have not shown differences in the coordination environment around Na with a varying Na/Si or Si/Al ratio (McKeown et al., 1985; Mazzara et al., 2000). On the other hand, recent quantum

* Author to whom correspondence should be addressed, at Geophysical Laboratory, Carnegie Institution of Washington, 5251 Broad Branch Rd., Washington DC, 20015 (s.lee@gl.ciw.edu).

chemical calculations support preferential interaction of Na^+ with different types of oxygens (bridging oxygens [BOs] vs. nonbridging oxygens [NBOs]) in the network (Uchino and Yoko, 1998) as well as with different types of BOs such as Al-O-Al and Si-O-Al.

Important progress in determining local Na^+ environments in glasses has been made through solid-state ^{23}Na NMR studies, which can provide several key aspects of the extent of disorder around both charge-balancing and charge-modifying cations (Oestrike et al., 1987; Xue and Stebbins, 1993). High-temperature NMR spectroscopy on melts has been particularly useful in yielding one of the structurally most relevant NMR parameters, the isotropic chemical shift (δ_{iso}), which is a sensitive probe of the local environment (George and Stebbins, 1996; Maekawa et al., 1997). ^{23}Na magic-angle spinning (MAS) NMR spectroscopy at multiple magnetic fields has been used to estimate average δ_{iso} values of silicate glasses (Gee and Eckert, 1996; Kohn et al., 1998; Ratai et al., 1998). Variations of ^{23}Na MAS NMR peak positions in aluminosilicate glasses and melts with respect to composition have been reported (Oestrike et al., 1987; Xue and Stebbins, 1993; George and Stebbins, 1996; Maekawa et al., 1997; Schmidt et al., 2000a). From the detailed analysis of δ_{iso} and atomic environments in crystalline silicates combined with recent ab initio molecular orbital calculations, several significant correlations between δ_{iso} and *d*(Na-O) (the mean first-shell distance), CN, net negative charge (or excess electron density, free valence) on oxygen, and bond valence sum have been reported (Xue and Stebbins, 1993; Koller et al., 1994; George and Stebbins, 1996; Tossell, 1998). Although there is relatively good correlation between average *d*(Na-O) and the isotropic chemical shift, it is important to note that the latter may result from the combination of several factors. For example, correlations between δ_{iso} and *d*(Na-O) show different trends for silicates, borates, germanates, and carbonates (Stebbins, 1998). In addition, the results from NMR spectroscopy on glasses are not in good agreement with those from other spectroscopic methods, including EXAFS (Houde-walter et al., 1993).

Although the average ^{23}Na δ_{iso} and thus the average local environment have been investigated, among the most fundamental aspects of glasses are the distributions of internal variables, including Na-O and other structural units, which are essential for modeling structure and properties. This kind of information has generally not been treated in detail in studies of glasses and is lost by motional averaging in high-temperature NMR spectroscopy. This difficulty of determining the chemical shift distribution and thus the distribution of internal variables from ^{23}Na NMR spectroscopy originates from the fact that ^{23}Na is a quadrupolar nuclide (spin 3/2) with a relatively large quadrupolar moment. The conventional MAS NMR spectra at lower fields, such as 7.1 and 9.4 T, are therefore severely broadened by second-order quadrupolar interactions (SQIs), masking the true distribution in δ_{iso}. One partial solution to this problem is to analyze MAS spectra at different fields to yield an estimate of the range in δ_{iso}, as was done recently for a series of Na aluminosilicate glasses (Schmidt et al., 2000a). MAS NMR spectroscopy at higher fields is especially helpful because the effect of SQIs decreases dramatically with increasing field (Kohn et al., 1998; Stebbins et al., 2000). Although high-field NMR spectroscopy cannot completely remove the effect of SQIs, the recent development of triple-quantum (3Q)MAS can be promising, even at lower fields, because it can yield distributions of both δ_{iso} and the quadrupolar coupling constant (C_q) (e.g., Lee and Stebbins, 2000b; Lee et al., 2001). ^{23}Na 3Q MAS NMR spectra free from quadrupolar broadening have proved to be very efficient in investigating short-range order in glasses and crystalline materials and can be a useful tool for exploring the local environment of Na, including Na-O distances, their compositional variation, and the existence of hydration products (Angeli et al., 1999, 2000; Egan and Mueller, 2000; Lim and Grey, 2000; Accardi et al., 2001). Recently, ^{23}Na 3Q MAS combined with structural correlation of NMR parameters was used to obtain Na-O distance distributions in several glasses, revealing that *d*(Na-O) varies with composition (Angeli et al., 2000).

This paper describes our investigation of the distribution of Na^+ in charge-balanced sodium aluminosilicate glasses (a model system for rhyolitic magmas) and binary sodium silicate glasses using solid-state ^{23}Na MAS NMR spectroscopy at varying fields (9.4, 14.1, and 18.8 T) and 3Q MAS NMR at 9.4 T. We explore the *d*(Na-O) distribution and its compositional dependence and present a model of Na distribution that is tied to the presently known ordering state of the aluminosilicate glasses. We then discuss the effect of Na environment and its distribution on the macroscopic properties of silicate melts. As far as we know, this is the first attempt to explore the *d*(Na-O) distribution in charge-balanced aluminosilicate glasses in terms of Na-BO interactions using the information from both ^{17}O and ^{23}Na NMR spectroscopy. We also report the first high-field (18.8 T) ^{23}Na MAS NMR spectra for sodium silicate glasses that are useful in the quantification of disorder.

2. EXPERIMENTAL

2.1. Sample Preparation

Sodium aluminosilicate glasses along the "charge-balanced" join with varying Si/Al (*R*) ratios ($NaAlSi_RO_{2R+2}$, where *R* ranges from 0.7 to 6) were synthesized from oxides (SiO_2, Al_2O_3) and carbonates (Na_2CO_3) by melting at 1873 K for 1 h and then by water quenching (for more detail, see Lee and Stebbins, 1999, 2000a, 2000b; Lee et al., 2001). Sodium silicate glasses with varying Na/Si ratios ($Na_2O \cdot SiO_2$ and $Na_2O \cdot 2SiO_2$) were also synthesized from these reagents by melting at 1673 K for ~1 hr. About 3% weight loss was observed for $Na_2O \cdot SiO_2$, presumably because of alkali volatilization. About 0.2% of cobalt oxide was added to all samples to reduce spin lattice relaxation times.

2.2. NMR Spectroscopy

^{23}Na MAS NMR spectra were collected at three magnetic fields (B_0) with a modified Varian-VXR400S spectrometer (9.4 T) at a Larmor frequency of 105.9 MHz and with Varian Inova 600 and Inova 800 spectrometers (14.1 and 18.8 T) at Larmor frequencies of 159 and 211.6 MHz, respectively. A 5-mm MAS probe (Doty Scientific, Inc.) was used to collect the spectra at 9.4 T, with a spinning speed of 14 to 15 kHz. At this field, the relaxation delay for ^{23}Na MAS NMR spectroscopy was 0.3 s, with a radio frequency pulse length of 0.25 μs, which is about a 15° tip angle for the central transition in solids. At 9.4 T, the shifted-echo pulse sequence (Baltisberger et al., 1996), composed of two hard pulses of durations of 5.3 and 1.8 μs, a selective pulse with a duration of 26 μs, and an echo time of ~0.8 ms, was used for the ^{23}Na 3Q MAS NMR experiment to ensure maximum intensity. A 3Q MAS NMR spectrum for crystalline Na_2HPO_4 was obtained under the same experimental conditions to estimate the C_q dependence of 3Q MAS efficiency (see below) (Medek et al., 1995).

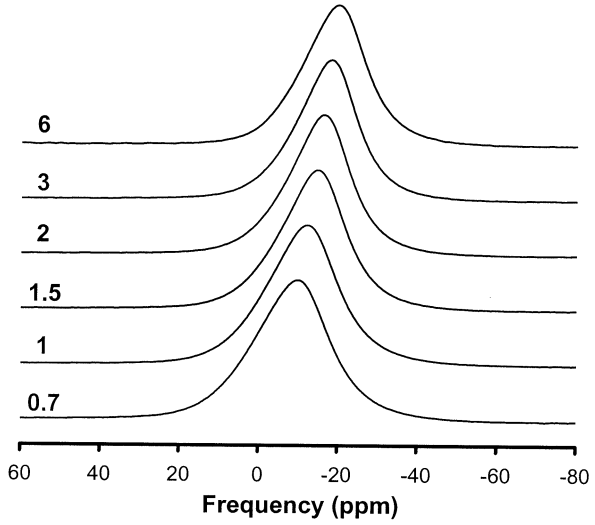

Fig. 1. ^{23}Na magic-angle spinning spectra of glasses on the $NaAlO_2$-SiO_2 join with varying Si/Al ratios (R) as labeled, collected at 14.1 T.

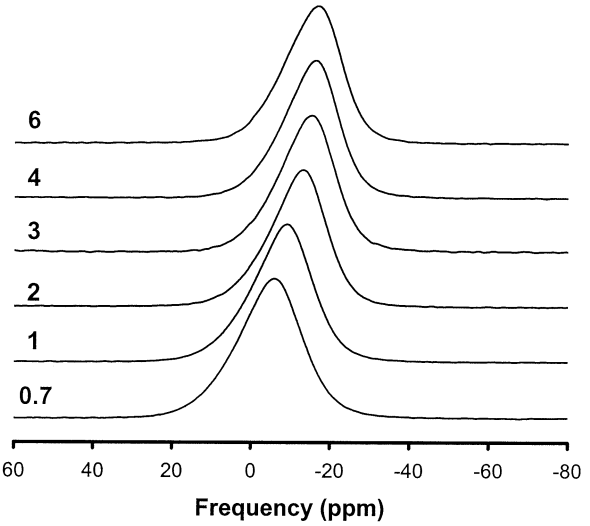

Fig. 2. ^{23}Na magic-angle spinning spectra of charge-balanced aluminosilicate glasses with varying R ratios as labeled (18.8 T).

At 14.1 T, a 3.2-mm Varian/Chemagnetics T3 MAS probe with a recycle delay of 0.1 s, a radio frequency pulse length of 0.2 μs, and spinning speed of 18 kHz was used for MAS experiments. ^{23}Na MAS spectra were also collected using a similar probe at 18.8 T. The recycle delay and the pulse length at 18.8 T were identical to those at 14.1 T and were determined to provide quantitative intensity information for Na sites with a distribution of quadrupolar parameters. The spinning speed at 18.8 T was 20 kHz. All spectra are referenced to 1-mol/L NaCl solution.

3. RESULTS AND DISCUSSION

3.1. ^{23}Na NMR Results for Aluminosilicate Glasses

Figure 1 illustrates the ^{23}Na MAS spectra of charge-balanced aluminosilicate glasses with varying Si/Al (R) at a relatively high field of 14.1 T. The peak maximum varies with composition from -10.3 ppm ($R = 0.7$) to -20.0 ppm ($R = 6$), consistent with systematic peak shifts as previously reported (Oestrike et al., 1987; Maekawa et al., 1997; Schmidt et al., 2000a). If we apply the inverse correlation between ^{23}Na δ_{iso} and average d(Na-O) established from crystalline silicates, d(Na-O) appears to increase with increasing Si content (see below for more discussion) (Xue and Stebbins, 1993; George and Stebbins, 1996). The line shapes show asymmetric extra intensity at higher frequencies (left side as plotted), which suggests that the chemical shift distribution is predominant over the quadrupolar broadening: the latter, relative to the former, scales inversely with the square of magnetic field. Figure 2 illustrates ^{23}Na MAS spectra of aluminosilicate glasses at 18.8 T that are only slightly narrower than those at 14.1 T and have similar shapes. At 18.8 T, the second-order quadrupolar broadening would contribute ~30% of the peak width for a typical C_q value of 2.5 MHz, confirming that the isotropic chemical shift distribution is predominant. Again, the peak maximum systematically moves toward lower frequencies with increasing R values from -5.9 ppm ($R = 0.7$) to–17.1 ppm ($R = 6$), probably because of the increasing Na-O distance or CN. The decreasing net negative charge on BOs as Si increases may also affect ^{23}Na δ_{iso}. The effect of quadrupolar broadening on the peak shape is more clearly manifested in spectra collected at 9.4 T, at which "tails" toward lower frequencies are obvious. This characteristic shape is due to the distributions of C_q and δ_{iso}. At this field, the peak maximum varies from -19.5 ppm ($R = 0.7$) to -27.6 ppm ($R = 6$) (Fig. 3).

Figure 4 shows the ^{23}Na MAS spectra for $NaAlSi_2O_6$ (jadeite composition) glass at a varying magnetic field from 9.4 to 18.8 T, summarizing the effects noted above: increasing field leads to narrowing of the peak width by reducing the broadening due to SQIs, as previously described (Kohn et al., 1998; Schmidt et al., 2000a). With values for ^{23}Na C_q of 1.5 to 3.5 MHz, typical for Na silicates, the quadrupolar broadening can be effectively reduced at 14.1 T if high spinning speeds such as

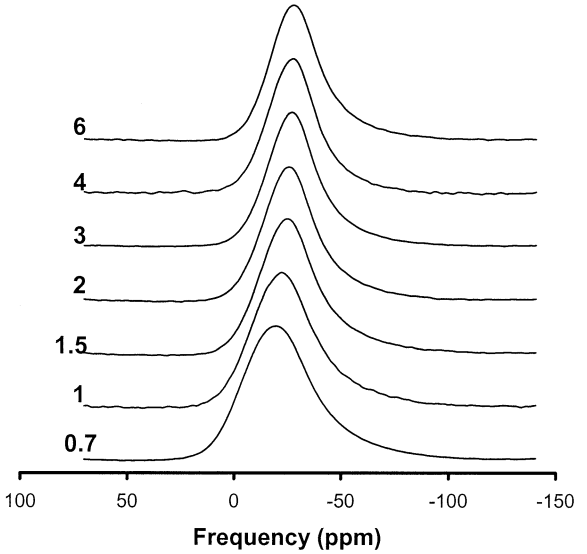

Fig. 3. ^{23}Na magic-angle spinning spectra of charge-balanced aluminosilicate glasses with varying R ratios as labeled (9.4 T).

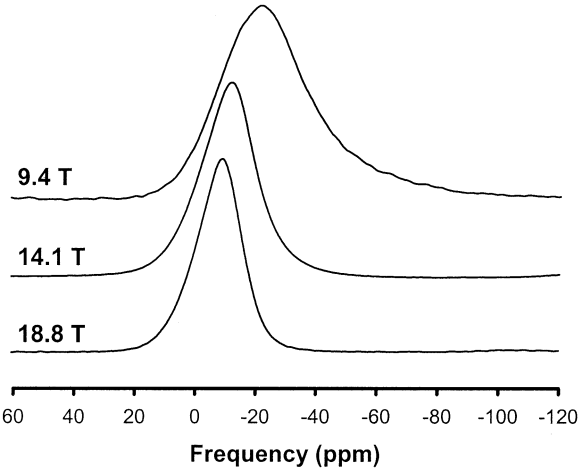

Fig. 4. ^{23}Na magic-angle spinning spectra for $NaAlSi_2O_6$ glass at 9.4, 14.1, and 18.8 T, showing dramatic reduction in quadrupolar broadening.

18 kHz are used, indicating that such spectra largely reflect real distributions of chemical shift. From the systematic variation of this distribution with composition, it can be deduced that the high-frequency tail is largely due to an increase in the number of Na environments with shorter *d*(Na-O), smaller CN, or increased proximity to BOs with larger free valence (such as Al-O-Al and Si-O-Al) with decreasing Si content. This type of skewness of the high-field spectra increases with increasing silica content, as shown in high-field data.

The variation of peak shape and position with composition is relatively large near to $R = 1$, which may reflect the relatively rapid variation in oxygen site populations (Si-O-Al, Si-O-Si, and Al-O-Al) in this range, as has been shown in our previous ^{17}O NMR study of aluminosilicate glasses (Lee and Stebbins, 2000a, 2000b). In addition, the peak widths (full width at half-maximum) of the spectra at higher fields (14.1 and 18.8 T) are only ~20 ppm, clearly revealing variations of peak shape and position with structural change. The observation that the Na^+ environment in charge-balanced aluminosilicate glasses strongly reflects the variation in BO population implies in turn that the distribution of Na^+ is relatively homogeneous throughout the framework, whose distributions are also homogeneous: if Na^+ showed a strong preference for sites surrounded only by Si-O-Al groups, for example, much less variation with Si/Al in the MAS spectra would be expected.

As mentioned above, although broadening due to SQIs is inherent in MAS NMR spectra, 3Q MAS NMR spectroscopy is particularly useful in eliminating this effect and can be done with a conventional MAS probe using a pulse sequence that produces a two-dimensional spectrum with correlation between multiple-quantum and single-quantum coherence. Figure 5 shows the ^{23}Na 3Q MAS NMR spectra for sodium aluminosilicate glasses. Here, the isotropic dimension is free of quadupolar broadening, but peak positions are controlled by both δ_{iso} and the quadrupolar coupling products (P_q) for given sites ($P_q = C_q\,[1 + \eta^2/3]^{1/2}$, where $0 \leq \eta \leq 1$ is the quadrupolar asymmetry parameter). It is clear that with increasing Si/Al, the chemical shift moves toward lower frequencies, consistent with ^{23}Na MAS spectra. At the same time, the width of distributions

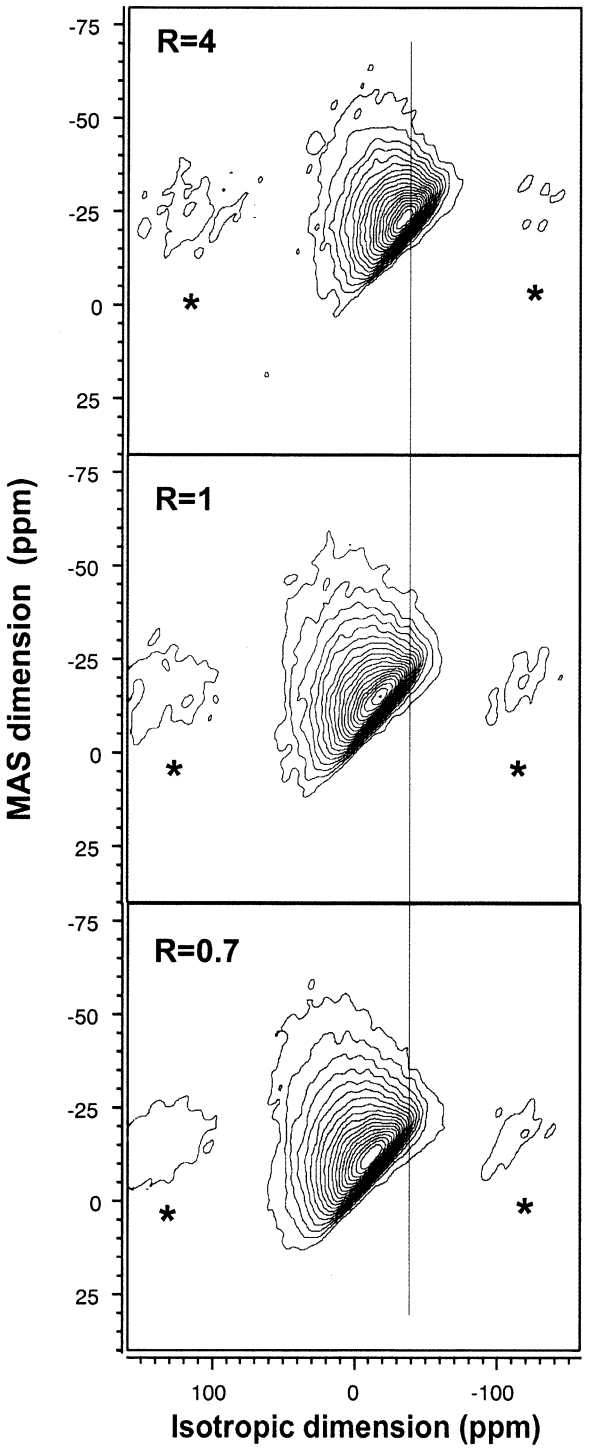

Fig. 5. ^{23}Na triple-quantum magic-angle spinning spectra of sodium aluminosilicate glasses with varying *R* ratios as labeled, collected at 9.4 T. Vertical line is to show shift in peak position, and asterisks refer to spinning side bands.

in δ_{iso} and C_q decrease slightly, as manifested in the widths of the spectra in both MAS and isotropic dimensions (Fig. 6). The local environment of Na thus varies with Si/Al, reflecting oxygen site populations, consistent with the MAS results. To more quantitatively utilize the 3Q MAS results, isotropic chem-

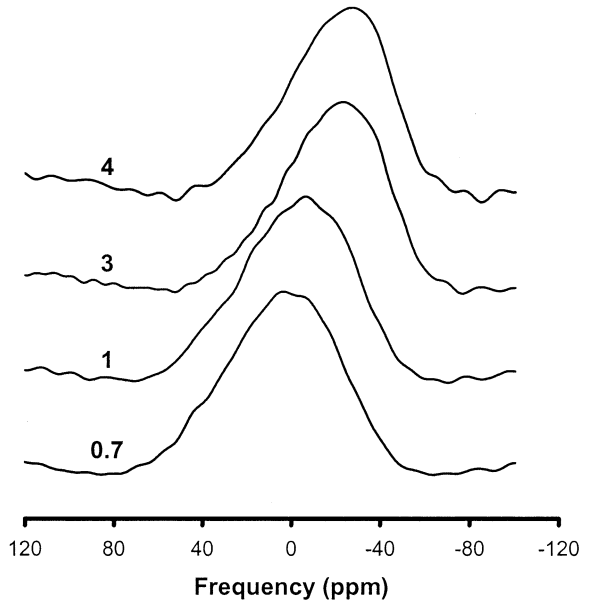

Fig. 6. Isotropic projection of ^{23}Na triple-quantum magic-angle spinning spectra, as in Figure 5, with *R* ratios as shown.

ical shift can be obtained from the center of gravity of the peak in both isotropic and 3Q MAS dimension (e.g., Lee and Stebbins, 2000b). In addition, 3Q excitation and reconversion efficiency depends significantly on the magnitude of the quadrupolar interactions, and therefore, it is necessary to calibrate the spectrum for quantification (Medek et al., 1995; Angeli et al., 1999). This process and the results are discussed in the next section.

3.2. Distribution of Charge-Balancing Cations in Aluminosilicate Glasses

As demonstrated above, ^{23}Na δ_{iso} is a strong function of composition, and high-field ^{23}Na MAS and 3Q MAS NMR spectroscopy can thus be effective probes for estimating not only average local environments but real distributions in structural parameters. A fundamental aspect of the inherent disorder in glasses and their precursor liquids is bond angle and length distribution that can contribute to the topological disorder in glasses and melts, affecting macroscopic transport properties, including viscosity and diffusivity of Na (Lee et al., 2001). Variation of δ_{iso} with Si/Al could be affected by structural variations with composition such as *d*(Na-O), CN, or the characteristics of the oxygens in the first shell such as the degree of underbonding, or by combination of these effects (Tossell, 1998). Here, we discuss the local environment of Na and attempt to obtain useful distribution functions of such internal variables.

In aluminosilicate glasses, changes with composition in Na oxygen coordination shells, including CN and bond angles (*T*-O-*T*, where *T* is the framework cation), are not well known. In particular, there is only limited experimental evidence for such changes with Si/Al (Oestrike et al., 1987; Xue and Stebbins, 1993; George and Stebbins, 1996; Maekawa et al., 1997; Schmidt et al., 2000a). For example, in recent Na- k-edge EXAFS studies, the Na environment appears to be rather invariant with composition (McKeown et al., 1985). On the other hand, molecular dynamics simulations of sodium aluminosilicate liquids showed that average T-O-T bond angle decreased with increasing Na content and decreasing *R*, suggesting a possible slight decrease in average CN with *R* (Scamehorn and Angell, 1991). Recent ^{23}Na MAS NMR spectroscopy for high-silica aluminosilicate glasses also shows a trend of increasing shielding with increasing Si, consistent with the results given here (Schmidt et al., 2000a, 2000b). Previous ^{23}Na NMR data on charge-balanced joins suggested that CN of Na in aluminosilicate liquids is ~7 to 8, dropping to 6 to 7 in Al-free sodium silicate gasses (George and Stebbins, 1996), while EXAFS results reported a CN of 5 for Al-free silicate glasses (Houdewalter et al., 1993; Mazzara et al., 2000). This noticeable discrepancy in CN values may be due to the processes associated with phase shift correction in EXAFS or the fact that ^{23}Na chemical shift is rather insensitive to CN, with significant overlap between CN values of 5 and 6 (Koller et al., 1994). Therefore, a more detailed look at the effect of the oxygen-bonding environment around Na is needed.

In aluminosilicate glasses on the $NaAlO_2$-SiO_2 join, the most obvious effects of silicate structure on δ_{iso} for ^{23}Na will be the type and distances of BO in the first shell. Recent ^{17}O NMR data clearly demonstrated that there are three different types of BO clusters (Si-O-Si, Si-O-Al, and Al-O-Al) whose populations are controlled by the degree of Al avoidance (*Q*) of ~0.94 as well as Si/Al (Lee and Stebbins, 2000a) (*Q* values of 1 and 0 refer to complete Al avoidance and random distribution of Si and Al, respectively.). Figure 7 shows ^{17}O MAS and 3Q MAS NMR spectra of $NaAlSiO_4$ glasses. Oxygen clusters are not well resolved in the MAS NMR spectrum because of quadrupolar broadening, whereas clear resolution among the different types of BOs is obvious in the ^{17}O 3Q MAS NMR data (Lee and Stebbins, 2000b). All three oxygen clusters interact with Na^+, as demonstrated by their variation of C_q and δ_{iso} with Na content (Lee and Stebbins, 2000b). That result also suggests that network "cages" comprising only a single type of oxygen cluster (e.g., Al-rich microsegregation) are negligible as well as that the probability of Na^+ located only in a single type of cage is low.

These three types of oxygen clusters have different amounts of excess negative charge and thus variable tendencies to donate electrons, which may have some effect on the ^{23}Na chemical shift depending on the number of different types of the clusters around a given Na^+ site. Quantum chemical calculation is useful to reveal the quantitative effect on δ_{iso} of changes in the oxygen free valence associated with NBO content (Tossell, 1998) as well as with Si/Al. On the other hand, a more obvious correlation between δ_{iso} and atomic configuration can be attributed to variation of the mean first shell distance, *d*(Na-O), on the basis of detailed analyses of data from crystalline silicates (George and Stebbins, 1996; Maekawa et al., 1997). A similar correlation can be made with data from only crystalline aluminosilicates, including nepheline (Na site), jadeite, anhydrous sodalite, albite (see Xue and Stebbins, 1993), and microcline (Phillips et al., 1988), yielding $\delta_{iso} = -64.4 \times d(\text{Na-O}) + 168.3$ ($R^2 = 0.984$) (Fig. 8). This correlation is similar to that used in a previous study (Angeli et al., 2000) for

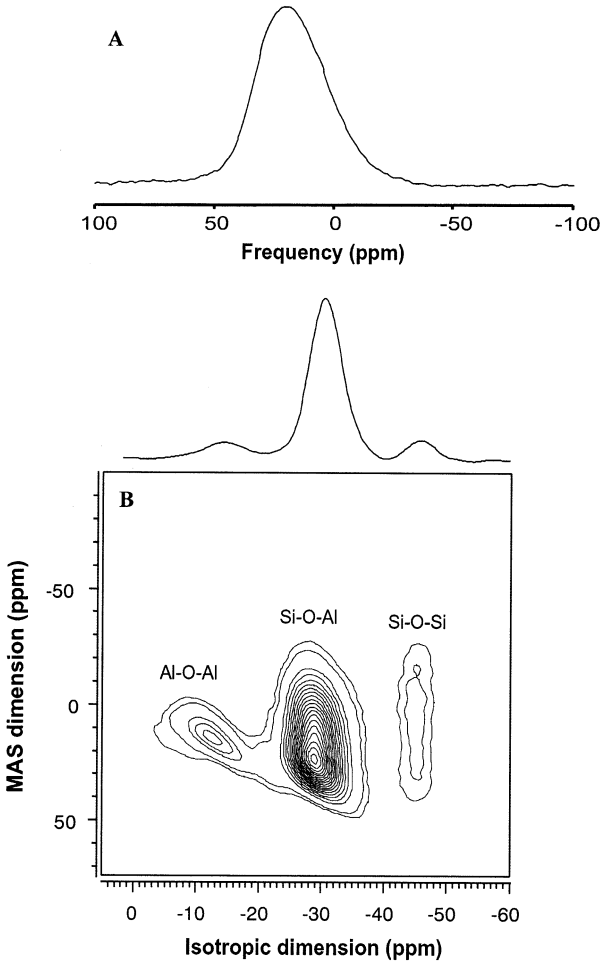

Fig. 7. Comparison of (A) ^{17}O magic-angle spinning (MAS) spectra and (B) triple-quantum MAS nuclear magnetic resonance spectra for $NaAlSiO_4$ glass (Lee and Stebbins, 2000a, 2000b). One-dimensional spectrum in (B) is the isotropic projection.

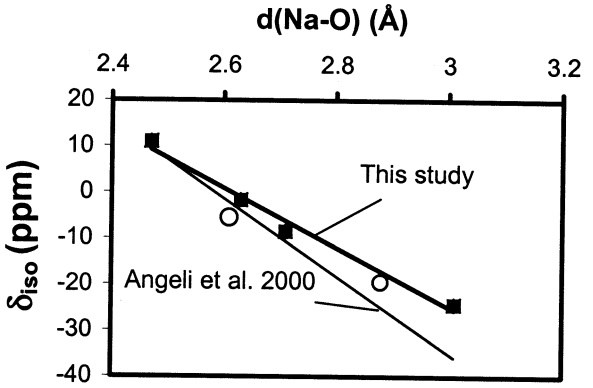

Fig. 8. ^{23}Na δ_{iso} vs. d(Na-O) for aluminosilicate glasses. Closed squares show data for jadeite, anhydrous sodalite, albite (data are from Xue and Stebbins, 1993) and microcline (Phillips et al., 1988). Open circles denote data for nepheline; Na^+ site (δ_{iso} and d[Na-O] of–5.5 ppm and 2.61 Å, respectively) and K^+ sites (−19.5 ppm and 2.88 Å). The data points from nepheline were not used because of uncertainty in structure and isotropic chemical shift (Stebbins et al., 1989). The correlation (thick solid line) is, however, close to these data points. Thin solid line is the trend line by Angeli et al. (2000).

the chemical shift range of aluminosilicate glasses (−15 ppm $< \delta_{iso} <$ 15 ppm). Therefore, in further analysis of chemical shift distributions, we assume that changes in δ_{iso} result only from variation in d(Na-O). Distributions in δ_{iso} thus depend on composition and reflect the change in d(Na-O) with composition.

As demonstrated in Figure 7 and in our previous ^{17}O NMR results, a major contribution to d(Na-O) distributions in sodium aluminosilicate glasses must be the variation of the relative population of different types of BOs around Na^+. In glasses with Na/Al > 1, variation in populations of BOs and NBOs will have similar effects. Recent ab initio molecular orbital calculations show that the greater interaction of Na^+ with more highly charged BOs leads to shorter Na-O distances for Al-O-Al than for Si-O-Si and thus affects the d(Na-O) distribution as a function of Si/Al. These theoretical results can be used to construct d(Na-O) distribution functions.

In spite of the improved resolution in 3Q MAS NMR spectra, peak intensities from this method are not quantitative unless corrected for the effect of varying C_q. 3Q MAS efficiency (3Q excitation and single-quantum conversion) depends on several factors, including radio frequency field strength and the magnitude of quadrupolar interactions. In particular, the dependency on the latter (C_q) of the intensity in the 3Q MAS experiment has been extensively studied (e.g., Vega and Noar, 1981; Medeck et al., 1995; Amoureux et al., 1996; Wu et al., 1996; Ding and McDowell, 1999; Lee and Stebbins, 2000b). Recent progress on quantification of 3Q MAS NMR spectra for oxide glass includes the full simulation of two-dimensional spectra with consideration of C_q dependence, thus obtaining distributions of NMR parameters (Charpentier et al., 1998; Angelli et al., 1999). Here, we use a method of quantification similar to that reported in our previous study (Lee and Stebbins, 2000b). The isotropic projections of the ^{23}Na 3Q MAS NMR spectra were corrected considering the variation of 3Q MAS efficiency with C_q using data from crystalline Na_2HPO_4, in which there are three Na sites with C_q values of ~1.4, 2.1, and 3.7 MHz and occupancies of 1:1:2, respectively (Fig. 9).

C_q values for Na environments in aluminosilicate glasses range from ~1.2 to 3.55 MHz from the ^{23}Na 3Q MAS NMR result obtained here, a range also comparable to that observed in crystalline silicates and aluminosilicates (Koller et al., 1994). It is thus likely that only small fractions of Na sites have smaller or larger C_q than the range covered by Na_2HPO_4, and thus this phase provides good constraints for this procedure. The fitted calibration function ($F[P_q]$) is $\exp(-[P_q - 0.8]/1.16)$. For further NMR data analysis, we assume that the quadrupolar asymmetry parameter (η) equals 0. The quadrupolar coupling product, P_q (C_q $[1 + \eta^2/3]^{1/2}$), therefore, is assumed to be identical to the quadrupolar coupling constant, C_q: variations of η from 0 to 0.5 and from 0.5 to 1 lead to differences of ~4 and 11%, respectively, between C_q and P_q.

We compared the experimental 3Q MAS efficiency for Na_2HPO_4 with that from numerical simulations using the software program Simpson (Bak et al., 2000), as shown in Figure 9. 3Q MAS efficiency from these two methods is similar for C_q ranges from 2 to 4 MHz but is rather different if C_q is < 2 MHz. It is thus important to check the validity of simulated 3Q

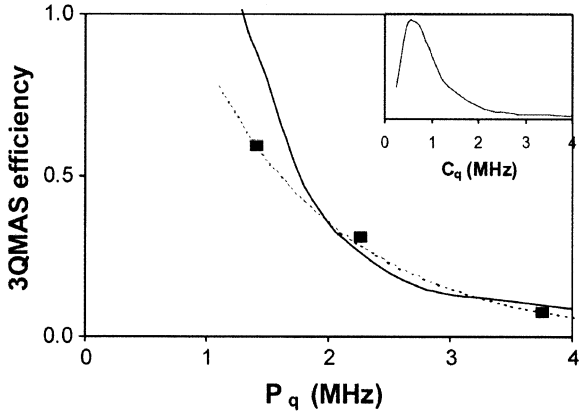

Fig. 9. Experimental dependence of triple-quantum magic-angle spinning (3Q MAS) efficiency on C_q for Na sites in Na_2HPO_4 (See text). Closed circles represent the experimental intensity of each site in Na_2HPO_4 relative to that expected from stoichiometry, and dotted line is fitting results (see text). Solid line denotes the 3Q MAS efficiency calculated using the software program Simpson (Bak et al., 2000) for spin 3/2 nuclei. Radio frequency field strength is 84 kHz, and all the simulation conditions are equivalent to the experimental setup (see section 2.2 in text), with a fixed η of 0. Solid line in inset shows the simulation results for the C_q ranges from 0.25 to 4 MHz.

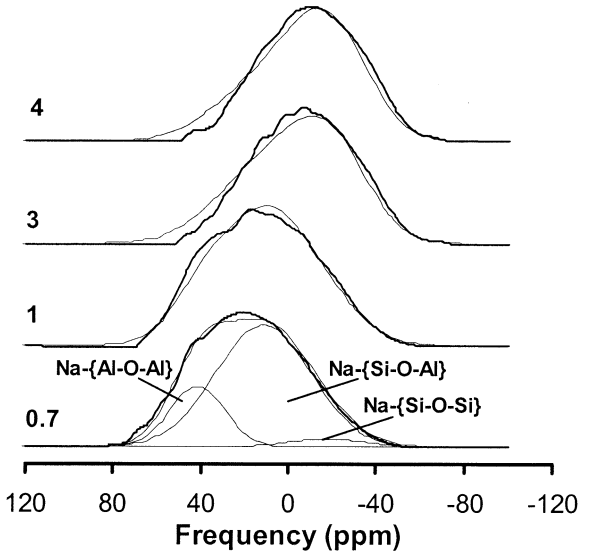

Fig. 10. Total isotropic projections of ^{23}Na triple-quantum magic-angle spinning (3Q MAS) spectra of aluminosilicate glasses with R ratios as shown, corrected for 3Q MAS efficiency (thick solid line, see text). Thin solid lines show gaussian components whose areas were obtained from ^{17}O nuclear magnetic resonance results and modeling (Lee and Stebbins, 2000a, 2000b).

MAS efficiencies using experiments on standard samples with known C_q values and site multiplicities, as was performed here and in our previous studies of other quadrupolar nuclide such as ^{27}Al and ^{17}O (Lee and Stebbins, 2000b).

Slices of the two-dimensional data, parallel to the MAS axis dimension in the 3Q MAS spectra, were taken and analyzed to yield estimates of C_q at each position in the isotropic dimension (δ_{3qmas}). Here, C_q values were obtained from the center of gravity in the MAS dimension (δ_{mas}) and the position of the slice assuming η of 0, as has been discussed (Baltisberger et al., 1996; Lee and Stebbins, 2000b); η is not well constrained by the broad, featureless projections in the MAS dimension of these types of spectra. From each two-dimensional NMR peak shape, it is rather clear that there is a systematic increase in C_q with increasing δ_{3qmas} that can be well approximated by single values of mean δ_{iso} and C_q at each δ_{3qmas}. This analysis leads to correlations among δ_{3qmas} and C_q as well as δ_{iso}. These results were used both to correct intensity and to convert 3Q MAS peak positions (δ_{3qmas}) to δ_{iso}. It should be mentioned that this approach of obtaining NMR parameters from the one-dimensional projections could be problematic if there are multiple sites with the same δ_{3qmas} and widely varying C_q values and hence very different intensity corrections. This appears not to be the case for the glasses studied here, although in principle, this possibility is allowed by the fact that δ_{3qmas} is a linear combination of C_q and δ_{iso}.

Figure 10 shows corrected intensity distributions in the 3Q MAS isotropic projections. We fitted data simultaneously for four compositions with three gaussians representing the contribution to mean d(Na-{T-O-T}), where T is Si or Al. Each fitted gaussian had a constant width and position, and the areas were constrained by ^{17}O 3Q MAS NMR spectroscopy and modeling of oxygen site population (Lee and Stebbins, 1999, 2002). This approach thus assumes that the average d(Na-{T-O-T}) is fixed with respect to composition for each BO type and that the probability of a given type of BO interacting with Na^+ depends only on the concentration of the oxygen cluster.

Figure 11 shows the average d(Na-O) distributions obtained from the ^{23}Na 3Q MAS NMR spectra using the correlation between δ_{iso} and average d(Na-O) from crystalline aluminosilicates. As expected, d(Na-O) increases with increasing Si content because of the increased faction of Si-O-Si, whose average distance from Na is longer than the average d(Na-{Si-O-Al}) and d(Na-{Al-O-Al}). The Na-O distributions are different for the three BO types, reflecting different distances and degrees of interaction. Figure 11B shows the individual components of the total distribution, which demonstrate that d(Na-{Al-O-Al}) at 2.52 ± 0.03 Å is shorter than d(Na-{Si-O-Si}) at ~2.81 ± 0.025 Å (Table 1). The most probable Na-{Si-O-Al} distance is intermediate at ~2.65 ± 0.025 Å. The mean distances obtained using a previous correlation (Angeli et al., 2000) are 2.54, 2.64, and 2.77 Å for Na-{Al-O-Al}, Na-{Si-O-Al}, and Na-{Si-O-Si}, respectively. The width of the distributions for Na-{Si-O-Si} and Na-{Si-O-Al} are almost identical, with standard deviations of ~0.1 Å. On the other hand, that for Na-{Al-O-Al} of ~0.05 Å is much narrower, suggesting a relatively high chemical affinity between Na and Al-O-Al, as has been shown in our recent quantum chemical calculations. The most probable d(Na-O) and its standard deviation for our $R = 1$ glass (~2.65 and 0.13 Å, respectively) are similar to the results for an $R = 1.5$ glass in a previous NMR study (~2.6 and 0.1 Å, respectively) (Angeli et al., 2000). This result is also consistent with average d(Na-O) from EXAFS data (~2.63 Å) (McKeown et al., 1985). Some EXAFS data using NaCl or $NaNO_3$ as a phase standard show an average Na-O distance of 2.3 Å (Mazzara et al., 2000). The d(Na-O) information obtained here is of course dependent on the δ_{iso} vs. d(Na-O) correlation used, and the effect of d(Na-O) on δ_{iso} may possibly be exaggerated by ignoring a contribution of the BO charge on

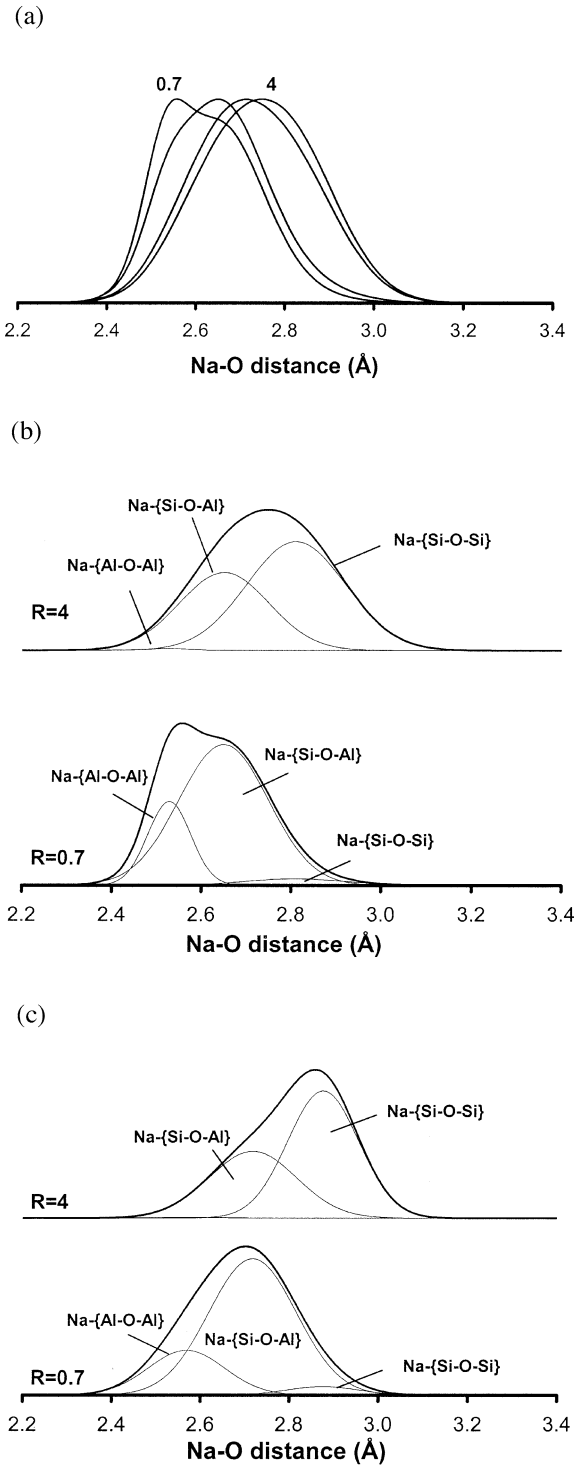

Fig. 11. (A) *d*(Na-O) distributions with *R* ratios as labeled in sodium aluminosilicate glasses obtained from ^{23}Na triple-quantum magic-angle spinning (3Q MAS) nuclear magnetic resonance spectra. (B) Contributions from each component for the samples. (C) *d*(Na-O) calculated from 3Q MAS spectra without considering effect of C_q on 3Q MAS efficiency.

δ_{iso}. Proper correction of 3Q MAS intensity is also important: Figure 11C shows *d*(Na-O) obtained without correction, for which the derived average *d*(Na-O) would be longer.

Table 1. Estimated Na-{*T*-O-*T*} distances from fitting of ^{23}Na triple-quantum magic-angle spinning spectrum for sodium aluminosilicate glasses. The standard deviation (σ) describes the width of the distribution, not uncertainty.

	d(Na-O) (Å)	σ (Å)
Na-{Si-O-Al}	2.65 (±0.025)	0.10 (±0.004)
Na-{Si-O-Si}	2.81 (±0.025)	0.10 (±0.004)
Na-{Al-O-Al}	2.52 (±0.03)	0.048 (±0.004)

Figure 12 illustrates the variation with Si/Al of ^{23}Na δ_{iso}, C_q, and average *d*(Na-O) (for all BOs), derived by the methods described above. Values of δ_{iso} are also compared with those obtained from the variation of the center of gravity of the MAS NMR peak (δ_{cg}) with B_0 (Schmidt et al., 2000a, 2001), which shows close similarity between the two methods. The δ_{iso} values derived here are in good agreement with results from aluminosilicate melts at high temperature, especially considering possible temperature effect on structure (Xue and Stebbins, 1993; George and Stebbins, 1996; Maekawa et al., 1997). On the other hand, our value for δ_{iso} of $NaAlSi_3O_8$ glass ($R = 3$, ~8 to 9 ppm) is less shielded than the value obtained in another recent study (Kohn et al., 1998), perhaps because the latter values were obtained at lower field than we used or because the small errors in δ_{cg} in either study could lead to a few parts per million variation, which can be accepted as the experimental uncertainty. C_q and δ_{iso} increase roughly linearly with X_{Al} (the mole fraction of Al relative to Al + Si), which implies that clustering among framework cations is unlikely, consistent with our previous results from ^{17}O NMR spectroscopy. Although ^{23}Na C_q is not as useful as δ_{iso} as a local probe of *d*(Na-O) and CN because of its sensitive variation with local site distortion (Koller et al., 1994), it is still interesting to observe that C_q also shows systematic variation with composition in this system. The results show that Na-O distance is strong function of composition and that Na^+ has different proximities to different types of BOs (Figs. 11 and 12C), suggesting that Na^+ distribution is not random. Here, a "random" distribution refers to the homogeneous distribution of Na^+ without any differential interaction with differing framework oxygens in a network that does not have microsegregation into Si- and Al-rich regions. Thus, we define a "perturbed" Na distribution in which Na distributes homogeneously and thus probes the types of BOs determined by composition and the degree of network disorder, but the distance between Na and these clusters reflects their reactivities. Such a distribution is distinct from a random Na distribution and from the "modified random network" (MRN) model in which Na^+ is clustered in regions rich in NBO or Al (Gaskell et al., 1991; Greaves and Ngai, 1995).

3.3. ^{23}Na NMR Results for Sodium Silicate Glasses and Distribution of Network-Modifying Cations

In some recent studies of Al-free silicate glasses, it has been proposed that Na^+ is mainly surrounded by NBO, forming Na-rich channels (MRN model) (Gaskell et al., 1991; Greaves and Ngai, 1995; Cormack and Du, 2001). Recent MD simulations, on the other hand, do not provide clear evidence for static

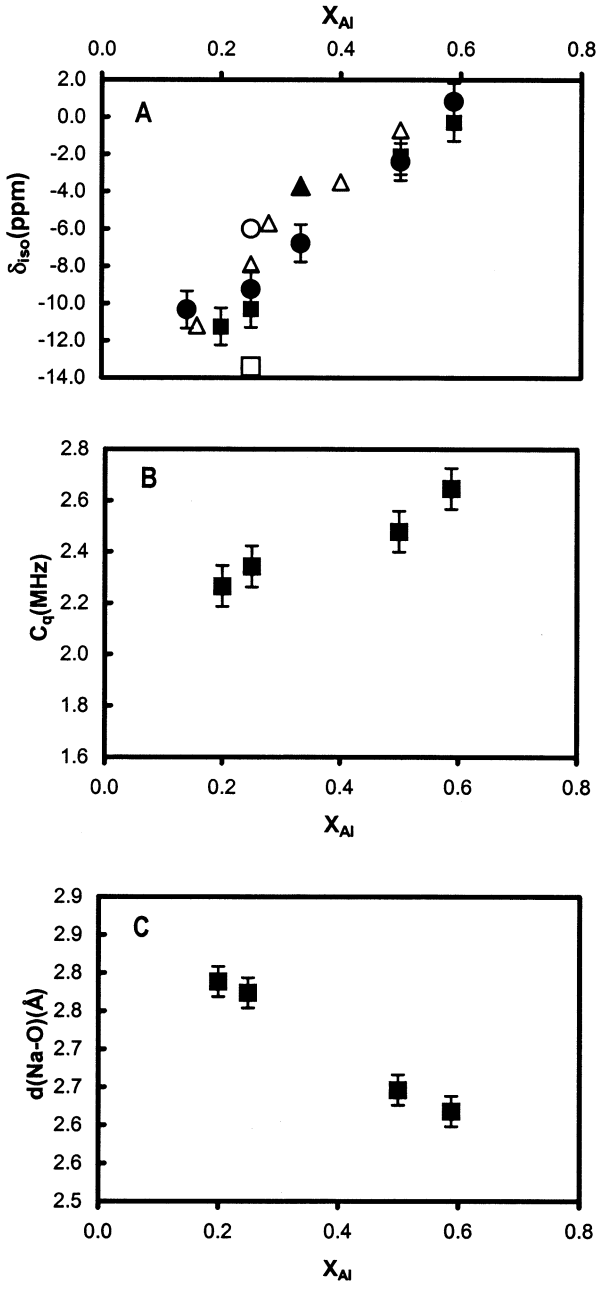

Fig. 12. Variation of (A) average δ_{iso}, (B) C_q, and (C) average d(Na-O) with composition (X_{Al} is the mole fraction of Al relative to Al + Si). Two different values of δ_{iso} were obtained, the first from ^{23}Na triple-quantum magic-angle spinning (MAS) (filled squares) and the second from ^{23}Na MAS nuclear magnetic resonance using the variation in the center of gravity with field (filled circles). Open square denotes the average δ_{iso} from Kohn et al. (1998). Open triangles refer to the data from Maekawa et al. (1997) for aluminosilicate melts. Filled triangle (X_{Al} = 0.33) and open circle (X_{Al} = 0.25) denote the data from Xue and Stebbins (1993) and George and Stebbins (1996), respectively.

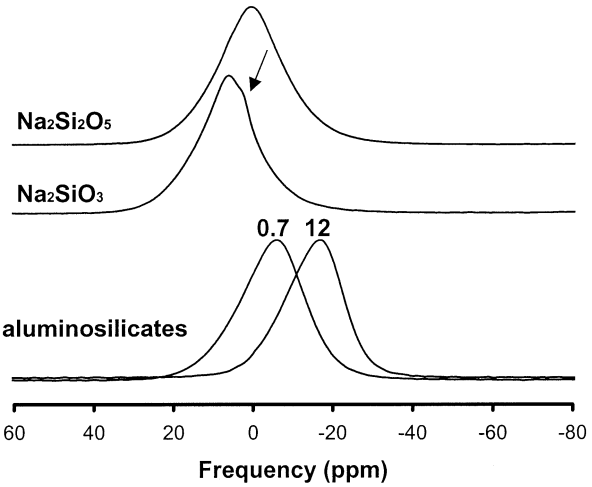

Fig. 13. ^{23}Na magic-angle spinning spectra of aluminosilicate glasses with R ratios as labeled and sodium silicate glasses collected at 18.8 T.

clustering of Na^+ (Jund et al., 2001). It is also possible that Na^+ can be near to some BO depending on the degree of disorder in the Na^+ distribution, either "random" or "perturbed." Systematic variations of NMR chemical shift with composition may thus provide some clue to Na^+ distributions in binary silicate glasses as well as aluminosilicate glasses. If Na^+ is mainly surrounded by NBO and increasing Na content only increases the volume fraction of the percolation channel (or alkali sublattice), the NMR chemical shift would not be expected to be strongly affected by the addition of Na unless the increasing fraction of percolation channel is due to increasing size (volume) of a single channel rather than increase in the number of channels with similar volume, which seems unlikely. On the other hand, if Na^+ sees both NBO and BO in the first shell, as suggested by "random" and "perturbed" distributions, increasing Na content should lead to an increase of δ_{iso} because the deshielding of Na increases with increasing negative charge on the oxygens coordinating Na^+ as the ratio of NBO to BO increases. Recent MD simulation and ab initio molecular orbital calculations also show that d(Na-NBO) is shorter than d(Na-BO) (Uchino and Yoko, 1998; Cormack and Du, 2001), indicating that the mean Na cage size and Na-O distance is likely to decrease with increasing Na, which will also tend to increase δ_{iso} in either of these scenarios.

Figure 13 shows the ^{23}Na MAS NMR spectra for binary sodium silicate and sodium aluminosilicate glasses at 18.8 T, at which peak shapes are dominated by the real chemical shift distributions. As previously reported at lower field, chemical shift increases with decreasing Na content and thus degree of polymerization (NBO/T) (Xue and Stebbins, 1993). Peak maxima in $Na_2O \cdot SiO_2$ (NS11, NBO/T = 2) and $Na_2O \cdot 2SiO_2$ (NS12, NBO/T = 1) glasses are ~6 and 0.4 ppm, respectively. The origin of small shoulder at ~2 ppm peak (Fig. 13, arrow) is not clear in NS11, but this feature may be due to an impurity resulting from absorption of H_2O and CO_2 in this hygroscopic glass. The Lorentzian peak shape for this spectrum may also reflect a relatively high Na^+ mobility. The ^{23}Na chemical shift range in sodium silicates is distinctly more "deshielded" (higher frequency) than that in sodium aluminosilicate glasses. The chemical shift variation with Na content in binary silicate glasses is intriguing because this trend seems to be consistent with the MRN model only if the size of individual Na^+ channels, and thus the size of the cage available for Na^+ decreases with increasing Na, which seems less likely. The data thus

appear to be consistent with either "random" or "perturbed" Na distributions, as discussed above.

As previously mentioned, the observed trend of increasing δ_{iso} with increasing Na/Si can be attributed to two factors. First, deshielding increases with increasing net negative charge on O as Na is coordinated by more NBO. Second, δ_{iso} increases because Na-NBO distances are likely to be smaller than Na-BO distances, although a previous EXAFS study could not detect significant variation of Na-O distance with composition (Mazzara et al., 2000). These results suggest that average *d*(Na-O) increases with increasing Si content in binary silicate glasses as average *d*(Na-O) increases with increasing Si in aluminosilicate glasses. This picture is clearly consistent with a "perturbed" Na distribution model; Na^+ can sample various oxygen environments such as Na surrounded by only NBO, by a fraction of NBO and BO, or mainly surrounded by BO whose fractions are dependent on BO/NBO, as Na^+ in aluminosilicate glasses in which Na^+ could be surrounded only by Al-O-Al or Si-O-Si, depending on composition.

The ^{23}Na 3Q MAS NMR spectra for binary sodium silicate glasses show some exaggerated features of hydration, making quantitative analysis similar to that for sodium aluminosilicate glasses difficult (Egan and Mueller, 2000). However, because MAS NMR peak shapes at 18.8 T roughly reflect the true δ_{iso} distribution, it can be shown that the fraction of Na-BO increases with increasing Si content (Fig. 13) in sodium silicate glasses (~66 and 40% Na-NBO in NS11 and NS12, respectively), and Na-BO appears to have longer distance than Na-NBO. Also, *d*(Na-{Si-O-Si}) in sodium silicate glasses appears to be shorter than that in sodium aluminosilicate glasses, as can be seen by the distinct chemical shift range between sodium silicate and aluminosilicate glasses at high *R*.

3.4. ^{23}Na δ_{iso} vs. Atomic Configurations in Aluminosilicate and Silicate Glasses and Dynamic and Static Properties of Silicate Melts

The observed relatively narrow ranges of chemical shift, quantified using the data from 3Q MAS NMR and MAS NMR spectroscopy at high static fields (14.1 and 18.8 T) show that Na^+ distribution in silicate glasses is not completely random. These methods can also be applied to other Na-containing oxide glasses to quantify the local configuration around Na and the extent of disorder among charge-balancing and modifying cations, which will eventually be helpful in establishing ^{23}Na chemical shift systematics, as has done for other nuclides, such as ^{29}Si. A more detailed discussion and extension to the other multicomponent silicate glasses will be given in a future contribution.

The distribution of Na^+ bonding environment is also clearly important to the static and dynamic properties of silicate melts, such as ionic diffusion and conductivity as well as viscosity. The structural disorder inherent in Na-O distance distributions gives insight into not only the spatial distribution of sodium in silicate glasses but the motions of Na^+. Na-O distance is an essential factor for ionic transport because it determines the binding energy that significantly contributes to the total activation energy barrier for Na transport. From the results given in this study, not only the average contribution to such energy barriers but also the distribution of energy barriers can be deduced. It should be noted that ionic transport is a complex function of several independent structural parameters including the number of available sites and density of Na^+, variations of the high-frequency dielectric constant, as well as long-range interactions (Greaves and Ngai, 1995). The spatial distribution of Na^+, as manifested as the *d*(Na-O) distribution, can also contribute to the topological entropy of sodium aluminosilicate glasses (Lee and Stebbins, 1999. This in turn contributes to the total configurational entropy of the system, which has been correlated with viscosity of silicate magmas through Adam-Gibbs theory (e.g., Richet, 1984). Other methods, such as X-ray absorption spectroscopy and quantum chemical calculations, can be potentially useful in providing constraints on Na distributions in silicate glasses that are critical in estimating these contributions (Greaves and Ngai, 1995).

4. CONCLUSIONS

Data from ^{23}Na MAS NMR spectroscopy at high field and 3Q MAS NMR spectroscopy at 9.4 T provide chemical shift data in sodium aluminosilicate glasses free from or with minimal second-order quadrupolar effects and are clearly an effective probe for local Na^+ ion environments and their distributions. The distributions of Na-O distances in sodium aluminosilicate glasses can be obtained from the distribution of δ_{iso} combined with previous studies of the disorder of Si and Al. ^{23}Na chemical shifts are mainly due to differences in *d*(Na-{*T*-O-*T*}) resulting from variations of the types of oxygen clusters around it, and the variation of bond length reflects the different degree of interaction between Na and each type of BO cluster. The *d*(Na-O) distribution functions show clear compositional dependence and manifests the differential reactivity between Na^+ and different types of bridging oxygens such as Si-O-Si, Si-O-Al, and Al-O-Al. The range of Na-O distances to each type of BO is relatively narrow, especially for Al-O-Al, suggesting less disorder than in traditional "random network" model. A similar trend can be found in binary silicate glasses, in which *d*(Na-BO) is apparently longer than the *d*(Na-NBO) but shorter than the *d*(Na-BO) in framework aluminosilicate glasses. This variation of isotropic chemical shift and *d*(Na-O) trend is consistent with a "perturbed" Na distribution model.

In this study, we provide new insights into the nature of disorder for non-network-forming cations in silicate glasses, which should contribute to a more complete, atomic-level understanding of the thermodynamic and dynamic processes in silicate magmas.

Acknowledgments—This project was supported by a Stanford Graduate Fellowship to S.K. Lee and by National Science Foundation grant EAR0104926. We are grateful to Professor J. Puglisi for access to, and Drs. L. Du and C. Liu for assistance with, the 18.8 T spectrometer in the Stanford Magnetic Resonance Laboratory. We also thank Professor G. E. Brown, Jr., for helpful discussions. We also thank Dr. Romano, Dr. Van Eck and one anonymous reviewer for the critical and helpful comments on the original manuscript.

Associate editor: C. Romano

REFERENCES

Accardi R. J., Lobo R. F., and Kalwei M. (2001) Paramagnetic effect of oxygen in the Na-23 MAS NMR and Na-23 MQMAS NMR spectroscopy of zeolite LiNaX. *J. Phys. Chem. B* **105,** 5883–5886.

Amoureux J. P., Fernandez C., and Frydman L. (1996) Optimized multiple-quantum magic-angle spinning NMR experiments on half-integer quadrupoles. *Chem. Phys. Lett.* **259,** 347–355.

Angeli F., Charpentier T., Faucon P., and Petit J. C. (1999) Structural characterization of glass from the inversion of Na-23 and Al-27 3Q-MAS NMR spectra. *J. Phys. Chem. B* **103,** 10356–10364.

Angeli F., Delaye J. M., Charpentier T., Petit J. C., Ghaleb D., and Faucon P. (2000) Influence of glass chemical composition on the Na-O bond distance: A Na-23 3Q-MAS NMR and molecular dynamics study. *J. Non-Cryst. Solids* **276,** 132–144.

Bak M., Rasmussen J. T., and Nielsen N. C. (2000) Simpson: A general simulation program for solid-state NMR spectroscopy. *J. Magn. Reson.* **147,** 296–330.

Baltisberger J. H., Xu Z., Stebbins J. F., Wang S., and Pines A. (1996) Triple-quantum two-dimensional ^{27}Al magic-angle spinning nuclear magnetic resonance spectroscopic study of aluminosilicate and aluminate crystals and glasses. *J. Am. Chem. Soc.* **118,** 7209–7214.

Charpentier T., Fermon C., and Virlet J. (1998) Numerical and theoretical analysis of multiquantum magic-angle spinning experiments. *J. Chem. Phys.* **109,** 3116–3130.

Cormack A. N. and Du J. C. (2001) Molecular dynamics simulations of soda-lime-silicate glasses. *J. Non-Cryst. Solids* **293,** 283–289.

Ding S. W. and McDowell C. A. (1999) Quantification of MQMAS spectra of solids containing quadrupolar nuclei. *Chem. Phys. Lett.* **307,** 215–219.

Egan J. M. and Mueller K. T. (2000) Detection and identification of corrosion products of sodium aluminoborosilicate glasses by Na-23 MQMAS and H-1 → Na-23 CPMAS NMR. *J. Phys. Chem. B* **104,** 9580–9586.

Gaskell P. H., Eckersley M. C., Barnes A. C., and Chieux P. (1991) Medium-range order in the cation distribution of a calcium silicate glass. *Nature* **350,** 675–677.

Gee B. and Eckert H. (1996) Cation distribution in mixed-alkali silicate glasses. NMR studies by Na-23-{Li-7} and Na-23-{Li-6} spin echo double resonance. *J. Phys. Chem.* **100,** 3705–3712.

George A. M. and Stebbins J. F. (1996) Dynamics of Na in sodium aluminosilicate glasses and liquids. *Phys. Chem. Min.* **23,** 526–534.

Greaves G. L. and Ngai K. L. (1995) Reconciling ionic-transport properties with atomic-structure in oxide glasses. *Phys. Rev. B* **52,** 6358–6380.

Houde-walter S. N., Inman J. M., Dent A. J., and Greaves G. N. (1993) Sodium and silver environments and ion-exchange processes in silicate and aluminosilicate glasses. *J. Phys. Chem.* **97,** 9330–9336.

Jund P., Kob W., and Jullien R. (2001) Channel diffusion of sodium in a silicate glass. *Phys. Rev. B* **64,** 4303–4308.

Kohn S. C., Smith M. E., Dirken P. J., van Eck E. R. H., Kentgens A. P. M., and Dupree R. (1998) Sodium environments in dry and hydrous albite glasses; improved ^{23}Na solid state NMR data and their implications for water dissolution mechanisms. *Geochim. Cosmochim. Acta* **62,** 79–87.

Koller H., Engelhardt G., Kentgens A. P. M., and Sauer J. (1994) ^{23}Na NMR spectroscopy of solids: Interpretation of quadrupole interaction parameters and chemical shifts. *J. Phys. Chem.* **98,** 1544–1551.

Lee S. K. and Stebbins J. F. (1999) The degree of aluminum avoidance in aluminosilicate glasses. *Am. Mineral.* **84,** 937–945.

Lee S. K. and Stebbins J. F. (2000a) Al-O-Al and Si-O-Si sites in framework aluminosilicate glasses with Si/Al=1: Quantification of framework disorder. *J. Non-Cryst. Solids* **270,** 260–264.

Lee S. K. and Stebbins J. F. (2000b) The structure of aluminosilicate glasses: High-resolution ^{17}O and ^{27}Al MAS and 3QMAS NMR study. *J. Phys. Chem. B* **104,** 4091–4100.

Lee S. K. and Stebbins J. F. (2002) The extent of inter-mixing among framework units in silicate glasses and melts. *Geochim. Cosmochim. Acta* **66,** 303–309.

Lee S. K., Musgrave C. B., Zhao P., and Stebbins J. F. (2001) Topological disorder and reactivity of borosilicate glasses: Ab initio molecular orbital calculations and ^{17}O and ^{11}B NMR. *J. Phys. Chem. B* **105,** 12583–12595.

Lim K. H. and Grey C. P. (2000) Characterization of extra-framework cation positions in zeolites NaX and NaY with very fast Na-23 MAS and multiple quantum MAS NMR spectroscopy. *J. Am. Ceram. Soc.* **122,** 9768–9780.

Maekawa H., Nakao T., Shimokawa S., and Yokokawa T. (1997) Coordination of sodium ions in $NaAlO_2$-SiO_2 melts: A high temperature Na-23 NMR study. *Phys. Chem. Min.* **24,** 53–65.

Mazzara C., Jupille J., Flank A. M., and Lagarde P. (2000) Stereochemical order around sodium in amorphous silica. *J. Phys. Chem.* **104,** 3438–3445.

McKeown D. A., Waychunas G. A., and Brown G. E. (1985) EXAFS and XANES study of the local coordination environment of sodium in a series of silica rich glasses and selected minerals within the Na_2O-Al_2O_3-SiO_2 system. *J. Non-Cryst. Solids* **74,** 325–348.

Medek A., Harwood J. S., and Frydman L. (1995) Mulitple-quantum magic-angle spinning NMR: A new method for the study of quadrupolar nuclei in solids. *J. Am. Chem. Soc.* **117,** 12779–12787.

Oestrike R., Yang W. H., Kirkpatrick R., Hervig R. L., Navrotsky A., and Montez B. (1987) High-resolution ^{23}Na, ^{27}Al, and ^{29}Si NMR spectroscopy of framework aluminosilicate glasses. *Geochim. Cosmochim. Acta* **51,** 2199–2209.

Phillips B. L., Kirkpatrick R. J., and Hovis G. L. (1988) Al-27, Si-29, and Na-23 MAS NMR study of an Al, Si ordered alkali feldspar solid-solution series. *Phys. Chem. Min.* **16,** 262–275.

Ratai E., Janssen M., and Eckert H. (1998) Spatial distributions and chemical environments of cations in single- and mixed alkali borate glasses: Evidence from solid state NMR. *Sol. St. Ion.* **105,** 25–37.

Richet P. (1984) Viscosity and configurational entropy of silicate melts. *Geochim. Cosmochim. Acta* **48,** 471–483.

Scamehorn C. A. and Angell C. A. (1991) Viscosity-temperature relations and structure in fully polymerized aluminosilicate melts from ion dynamic simulations. *Geochim. Cosmochim. Acta* **55,** 721–730.

Schmidt B. C., Riemer T., Kohn S. C., Behrens H., and Dupree R. (2000a) Different water solubility mechanisms in hydrous glasses along the Qz-Ab join: Evidence from NMR spectroscopy. *Geochim. Cosmochim. Acta* **64,** 513–516.

Schmidt B. C., Riemer T., Kohn S. C., Behrens H., and Dupree R. (2000b) Different water solubility mechanisms in hydrous glasses along the Qz-Ab join: Evidence from NMR spectroscopy (vol 64, pg 513, 2000). *Geochim. Cosmochim. Acta* **64,** 2895–2896.

Schmidt B. C., Riemer T., Kohn S. C., Behrens H., and Dupree R. (2001) Structural implications of water dissolution in haplogranitic glasses from NMR spectroscopy: Influence of total water content and mixed alkali effect. *Geochim. Cosmochim. Acta* **65,** 2949–2964.

Stebbins J. F. (1998) Cation sites in mixed-alkali oxide glasses: Correlations of NMR chemical shift data with site size and bond distance. *Sol. St. Ion.* **112,** 137–141.

Stebbins J. F., Farnan I., Williams E. H., and Roux J. (1989) Magic angle spinning NMR observation of sodium site exchange in nepheline at 500°C. *Phys. Chem. Min.* **16,** 763–766.

Stebbins J. F., Kroeker S., Lee S. K., and Kiczenski T. J. (2000) Quantification of five- and six-coordinated aluminum ions in aluminosilicate and fluoride-containing glasses by high-field, high-resolution Al-27 NMR. *J. Non-Cryst. Solids* **275,** 1–6.

Tossell J. A. (1998) Quantum mechanical calculation of Na-23 NMR shieldings in silicates and aluminosilicates. *Phys. Chem. Min.* **27,** 70–80.

Uchino T. and Yoko T. (1998) Structure and vibrational properties of sodium disilicate glass from ab initio molecular orbital calculations. *J. Phys. Chem. B* **102,** 8372–8378.

Vega S. and Noar Y. (1981) Triple quantum NMR on spin systems with I=3/2 in solids. *J. Chem. Phys.* **75,** 75–86.

Wu G., Rovnyank D., Sun B., and Griffin R. G. (1996) High-resolution multiple quantum MAS NMR spectroscopy of half-integer quadrupolar nuclei. *Chem. Phys. Lett.* **249,** 210–217.

Xue X. and Stebbins J. F. (1993) ^{23}Na NMR chemical shifts and the local Na coordination environments in silicate crystals, melts, and glasses. *Phys. Chem. Min.* **20,** 297–307.